ACS APPLIED MATERIALS & INTERFACES

Research Article

www.acsami.org

Highly Enhanced Force Generation of Ionic Polymer–Metal Composite Actuators via Thickness Manipulation

Jong Hyuk Park,*[,†] Sung Won Lee,[‡] Dae Seok Song,[‡] and Jae Young Jho*[,‡]

[†]Photo-Electronic Hybrids Research Center, Korea Institute of Science and Technology, Seoul 136-791, Korea

[‡]School of Chemical and Biological Engineering, Seoul National University, Seoul 151-744, Korea

Supporting Information

ABSTRACT: On purpose to enhance the generating force of ionic polymer–metal composite (IPMC) actuators, the thickness of the ion-exchange membrane is manipulated in two different ways. One is grafting poly(styrenesulfonic acid) onto poly(vinylidene fluoride-*co*-hexafluoropropylene) films with varying thickness, and the other is stacking pre-extruded Nafion films to thicker films by pressing at high temperatures. For both groups of the membranes, ionic properties including ion-exchange capacity and ionic conductivity are maintained similarly inside the groups regardless of the thickness. The actuation tests clearly show the increase in generating force with increasing thickness of the IPMCs prepared. It is due to a larger bending stiffness of thicker IPMCs, which is consistent with the predicted result from the cantilever beam model. The increase in force is more remarkable in Nafion-stacked IPMCs, and a thick IPMC lifts a weight of 100 g, which far exceeds the reported values for IPMCs.

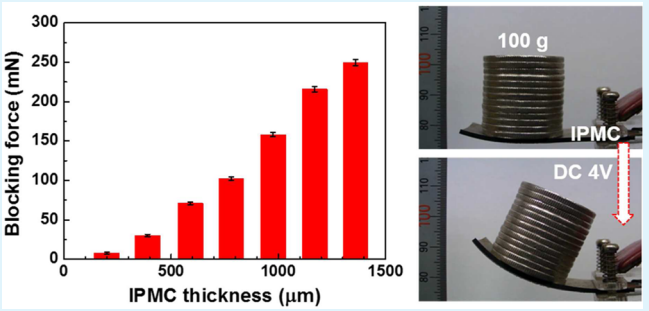

KEYWORDS: *ionic polymer–metal composite, actuator, electroactive polymer, force generation, ion-exchange membrane, thickness manipulation*

1. INTRODUCTION

Ionic polymer–metal composites (IPMCs) are a kind of electroactive polymers that exhibit shape or volume changes in response to electrical stimulation.[1] IPMCs comprise an ion-exchange membrane with two metal electrodes plated on the surface.[2−4] When applying electric potential to the electrodes, the mobile ions combined with water molecules are drawn to the electrodes by electrostatic force. The movement of the hydrated ions induces the changes in volume of the ion-exchange membranes, resulting in the actuation of IPMCs.[3,5] Because IPMCs can show a large bending strain and a prompt response under low applied voltages, they have considerable potential in developing artificial muscles for robotic, biomedical, and aerospace fields.[6,7]

However, the application of IPMCs has been restricted because of their insufficient force generation. Many efforts have been devoted to address this issue.[7] First of all, the structure and morphology of the metal electrodes were improved by using electroplated layers,[8] buffer layers,[9] and nanothorn electrodes,[10] leading to the reduced surface resistance and enhanced capacitive properties of the electrodes. In addition, the ion-exchange membranes were reinforced by incorporating them with nanoparticles, such as carbon materials[11−14] and silicates,[15,16] thus providing the improved mechanical and electrical properties for the membranes. Despite some progress being achieved, the maximum weight lifted by IPMC actuators in the actual demonstration reached only about 7.7 g,[17] which still needs to be improved in order to be pertinent for a wide variety of practical applications. Therefore, it is necessary to develop IPMC actuators with a highly enhanced force generation.

One method to improve the force of IPMCs is related to the thickness manipulation of ion-exchange membranes, which determine the dimensions of IPMCs. IPMCs, with well-designed dimensions, can be beneficial in generating a large force. Indeed, it has been experimentally proven that the increase in the membrane thickness imparts an enhanced force to the IPMCs.[18] However, because most IPMCs have been fabricated with thin pre-extruded ion-exchange membranes, for example, Nafion and Flemion, the thickness of the resulting IPMCs has been limited to less than 500 μm, causing low force generation.[19−22] Although a few ion-exchange membranes prepared via solution casting exhibited increased thickness,[17,23,24] the method does not seem to be convenient because of the low reproducibility and long duration for casting membranes. Consequently, a simple, reproducible, and scalable procedure for controlling the thickness of ion-exchange membranes is still needed to enhance the force generation of IPMC actuators.

Received: May 18, 2015
Accepted: July 15, 2015
Published: July 15, 2015

DOI: 10.1021/acsami.5b04296
ACS Appl. Mater. Interfaces 2015, 7, 16659−16667

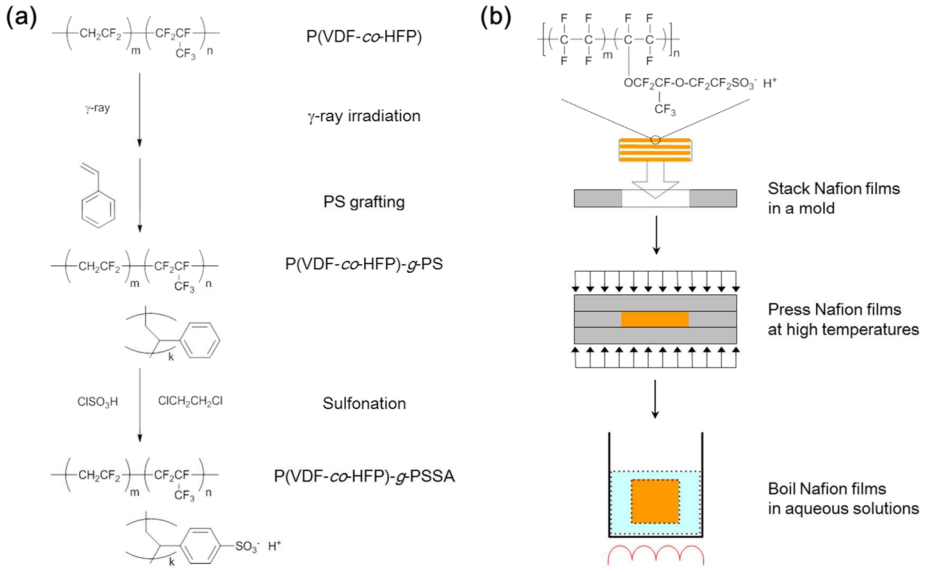

Figure 1. Schematic for two approaches to prepare ion-exchange membranes with different thicknesses. (a) P(VDF-*co*-HFP)-*g*-PSSA membranes obtained by a γ-ray-induced grafting method and (b) Nafion films stacked by pressing at high temperatures.

Herein, two favorable methods are suggested to obtain the ion-exchange membranes with desired thickness. One is radiation-induced graft copolymerization of ionic monomers onto fluoropolymer films,[25] and the other is stacking of pre-extruded ion-exchange membranes via pressing at high temperatures.[18] Both processes provide ion-exchange membranes with controlled thickness as well as uniform distribution of ionic groups through the entire thickness. The resulting membranes are employed for IPMC actuators, whose performance is systematically characterized. This approach demonstrates that manipulating the thickness of IPMC actuators is an effective route to their enhanced force generation, allowing their expanded use for a variety of practical applications.

2. EXPERIMENTAL SECTION

2.1. Materials. The following were purchased from Aldrich: poly(vinylidene fluoride-*co*-hexafluoropropylene) [P(VDF-*co*-HFP), M_n = 130000], styrene (99%), chlorosulfonic acid (99%), 1,2-dichloroethane (99%), tetraammineplatinum(II) chloride hydrate (98%, $[Pt(NH_3)_4]Cl_2{\cdot}xH_2O$), sodium borohydride (98%), sodium carbonate (99%), a sodium hydroxide standard solution (0.1 M), and a hydrochloric acid standard solution (0.1 M). Pre-extruded Nafion 117 films were obtained from DuPont. Styrene was purified by distillation under reduced pressure. All the other chemicals were used without further purification.

2.2. Radiation Grafting. P(VDF-*co*-HFP) was molded into films with thicknesses of 100, 200, and 550 μm by using a hot press. Under a nitrogen atmosphere at room temperature, the films were irradiated with γ-rays using a ^{60}Co source.[25,26] The irradiation rate was 7.0 kGy·h^{-1}. The absorbed dose for each film was varied as follows: 30 kGy for 100- and 200-μm-thick films and 50 kGy for 550-μm-thick ones.

For graft polymerization, the irradiated films were immersed in purified and nitrogen-purged styrene at 70 °C. The grafting time for each film was adjusted as follows: 8 h for 100- and 200-μm-thick films and 16 h for 550-μm-thick ones. The resulting films were Soxhlet-extracted with chloroform for 6 h to remove the residual monomer and polystyrene (PS) homopolymer. After the grafted films were dried to a constant weight, the degree of grafting (DOG) was determined as follows:

$$\mathrm{DOG}(\%) = \frac{W_g - W_i}{W_i} \times 100$$

where W_g and W_i are the weights of the grafted and initial films, respectively.

To offer ionic groups to styrene, the PS-grafted films were swollen in 1,2-dichloroethane for 24 h and then sulfonated by soaking in a 0.5 M chlorosulfonic acid/1,2-dichloroethane solution for 48 h. The sulfonated films were rinsed with ethanol several times, followed by boiling in deionized water for 6 h.

2.3. Stacking of Nafion Films. To find the optimal conditions for stacking Nafion films, the thermal behavior of Nafion, depending on temperature, was characterized by using thermogravimetric analysis (TGA) and differential scanning calorimetry (DSC). Both curves were recorded at a heating rate of 10 °C/min under nitrogen atmosphere. The chemical structure of the pristine Nafion film and the stacked one was analyzed by using Raman spectroscopy with a Nd:YAG laser.

Nafion 117 films were cut into proper dimensions (~70 × 70 mm^2), and the surfaces were cleaned with *n*-hexane. The films were piled in a stainless steel mold, and the thickness of the product was controlled by varying the number of the stacked layers. The mold was placed between preheated presses at 190 °C for 30 min, and then a pressure of ~40 MPa was applied at the same temperature for 10 min. After cooling to room temperature, the resulting membrane was boiled at 100 °C for 1 h in the following aqueous solutions in sequence: 10 wt % of hydrochloric acid, 10 wt % of hydrogen peroxide, and deionized water.

2.4. Characterization of the Membrane Properties. The distribution of sulfonate groups in the ion-exchange membranes obtained via radiation grafting and film stacking was observed by using energy-dispersive spectroscopy (EDS).

To quantify water uptake, the ion-exchange membranes were dried to a constant weight and followed by sufficient hydration with deionized water. The water uptake is defined as follows:

$$\text{Water uptake(g/g)} = \frac{W_{wet} - W_{dry}}{W_{dry}}$$

where W_{wet} and W_{dry} are the weights of the wet and dry membranes, respectively.

To evaluate the ion-exchange capacity (IEC), the membranes were dried to a constant weight and then immersed in a known volume of a 0.1 M sodium hydroxide solution for 48 h. The protons in the membranes were thoroughly exchanged for sodium ions. The amount of the protons was quantified by titration of the exchanged solution with a 0.1 M hydrochloric acid solution. IEC is calculated as follows:

DOI: 10.1021/acsami.5b04296
ACS Appl. Mater. Interfaces 2015, 7, 16659−16667

Table 1. Properties of Produced Ion-Exchange Membranes

material	denotation	thickness (μm)	DOG (%)	IEC (meq·g^{-1})	water uptake (g·g^{-1})	ionic conductivity (mS·cm^{-1})
P(VDF-*co*-HFP)-*g*-PSSA	TN	260	96	2.86	2.01	159
	MI	530	93	2.83	1.94	156
	TK	1280	98	2.76	1.90	151
Nafion	1L	190		0.91	0.22	15
	3L	570		0.92	0.23	18
	5L	955		0.91	0.24	18
	7L	1340		0.91	0.25	19

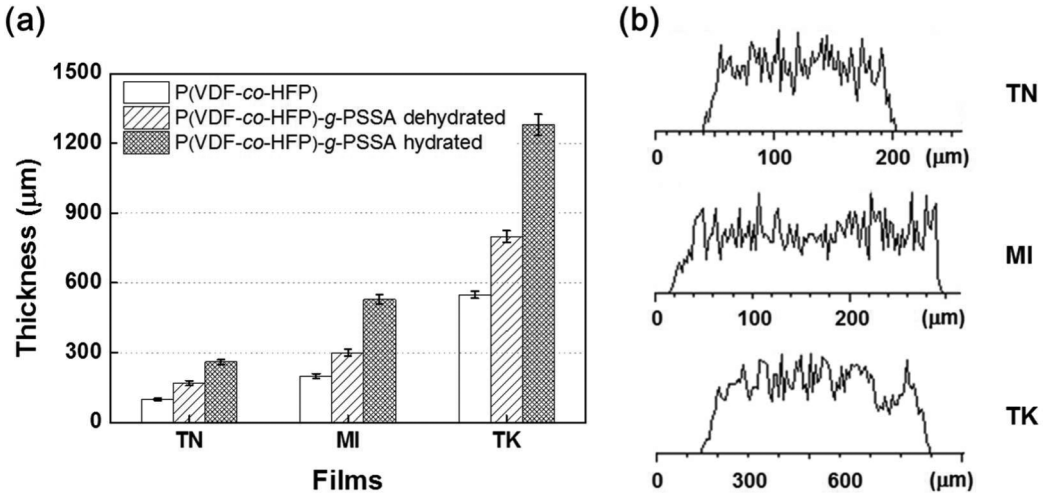

Figure 2. (a) Thickness change of P(VDF-*co*-HFP) films by radiation grafting and hydration. (b) Sulfur profiles through the thickness of the P(VDF-*co*-HFP)-*g*-PSSA membranes with different thicknesses.

$$\mathrm{IEC(meq/g)} = \frac{M_{ex}}{W_{dry}}$$

where M_{ex} is the number of moles of the exchanged ions in the membrane, and W_{dry} is the weight of the dried membrane.

To measure ionic conductivity, the membranes were fully hydrated with a 0.1 M aqueous solution of sodium carbonate. It enables the mobile ions in the membranes converted into sodium ions, which also occurs under the conditions of real actuation. The membranes were cut into a size of 10 × 40 mm^2 and then mounted onto the conductivity cell with a four-point probe. The impedance analyzer was operated in galvanostatic mode with a current amplitude of 0.01 mA over the frequency range from 1 MHz to 10 mHz using the Nyquist method.[27]

To observe the structure of ionic clusters in the membranes, small-angle X-ray scattering (SAXS) measurements were conducted with Cu K-alpha radiation (λ = 0.154 nm). For the measurements, the membranes containing mobile ions of H^+ were sufficiently hydrated with deionized water.

2.5. Fabrication of IPMCs. IPMCs were fabricated with the ion-exchange membranes prepared through radiation grafting and film stacking. The membranes with a size of 50 × 50 mm^2 were sufficiently soaked in a 0.5 wt % aqueous solution of tetraammineplatinum chloride hydrate and then placed in a bath containing 300 mL of deionized water at 40 °C. A 5 wt % aqueous solution of sodium borohydride was utilized as a reducing agent to form platinum layers on both surfaces of the membranes. Five milliliters of the solution was added to the water bath with stirring every 30 min. In order to provide the metal electrodes with a constant thickness for all IPMCs, regardless of their membrane thickness, the total amount of the added solution was regulated.

2.6. Actuation of IPMCs. For characterization of the actuation properties, the mobile ions in IPMCs were exchanged for sodium ions by soaking them in a saturated aqueous solution of sodium carbonate for 24 h. The IPMCs were cut into strips with a standard dimension (5 mm in width and 40 mm in length) and then mounted on a laser displacement meter incorporated with a load cell (Figure S1 in the Supporting Information). The displacement and blocking force of IPMCs were observed under direct current (DC) and alternating current (AC) voltages. When measuring the actuation properties, the applied potential (2, 3, or 4 V) and detection point (10, 15, or 20 mm away from the grip) were chosen for each IPMC; in this way, the displacement and blocking force of IPMCs could be more distinct.

3. RESULTS AND DISCUSSION

3.1. Preparation of Ion-Exchange Membranes. Figure 1 describes two different methods to provide ion-exchange membranes with controlled thickness. One route is radiation grafting. It has been shown that radiation grafting can be an effective approach to prepare ion-exchange membranes with designated ionic groups either cationic or anionic and thus IPMCs exhibiting improved performance.[25,26] In addition, radiation grafting can easily produce large-area ion-exchange membranes[28,29] which lead to a low-cost and high-throughput process for the fabrication of IPMCs. The radiation grafting is usually performed as follows.[30,31] A base polymer is irradiated with γ-rays to create radicals. Next, the radicals are reacted with monomers, resulting in the graft polymerization of monomers onto the base polymer. Finally, the grafted polymers are functionalized to offer ionic groups. In this study, P(VDF-*co*-HFP) was selected as a base polymer in virtue of its good mechanical properties and high radiation resistance.[30,31] Sulfonate groups, the most commonly used ionic groups for IPMCs,[7,19] were introduced into the ion-exchange membranes by styrene grafting and sulfonation. As a result, poly(styrenesulfonic acid) (PSSA)-grafted P(VDF-*co*-HFP) [P(VDF-*co*-HFP)-*g*-PSSA] ion-exchange membranes were ob-

DOI: 10.1021/acsami.5b04296
ACS Appl. Mater. Interfaces 2015, 7, 16659−16667

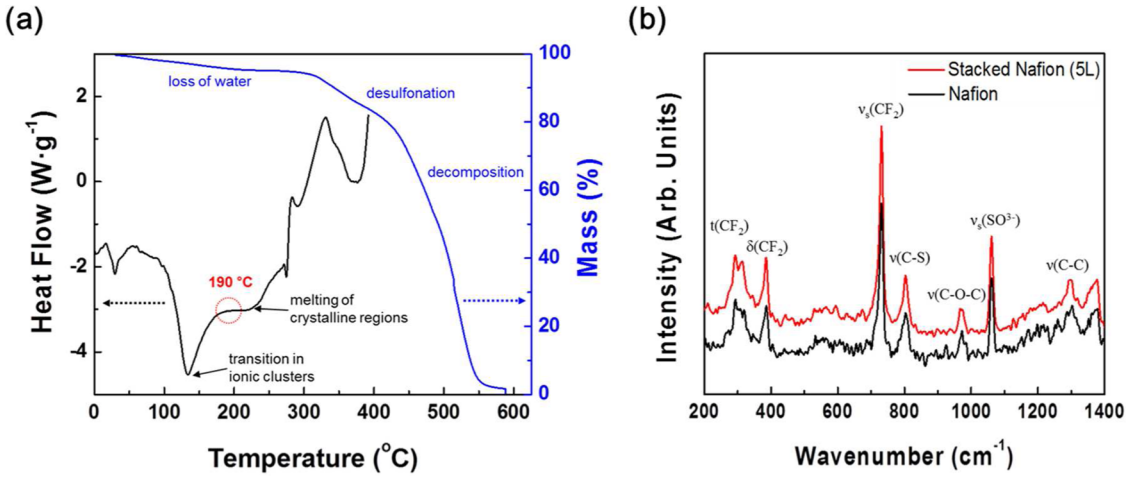

Figure 3. (a) DSC (black) and TGA (blue) curves of Nafion 117 films containing mobile ions of H^+. (b) Raman spectra of Nafion 117 (1L) and stacked Nafion films (5L).

tained as shown in Figure 1a. The amount of ionic groups in the resulting membranes can be regulated by varying the grafting conditions.[26,32] Moreover, unless the base polymer is not extremely thick, the ionic groups can be evenly distributed in the entire membranes. Consequently, this radiation-grafting method allows the prepared ion-exchange membranes with different thicknesses to contain the same amount of ionic groups per unit volume.

The other route to manipulate the thickness of ion-exchange membranes is stacking of pre-extruded membranes. Nafion is the most representative material for ion-exchange membranes of IPMCs. However, the thickness of most Nafion films has been limited to less than 500 μm. While solution-cast Nafion films showed an increased thickness, it was difficult to prepare uniform membranes with a large area. In addition, the long duration for film casting led to low productivity.[17,33] Fortunately, it has been demonstrated that Nafion films can be stacked via pressing at high temperatures (Figure 1b).[18] Through varying the number of stacked layers, the thickness of the resulting films can be readily controlled without the variation of the other membrane properties.

3.2. Properties of Radiation-Grafted Ion-Exchange Membranes. P(VDF-*co*-HFP) films, with three different thicknesses of 100, 200, and 550 μm, were utilized as the base polymer for radiation grafting. The radiation dose and grafting time for each film were controlled to give identical DOG values to all three films regardless of their initial thickness. The DOG values for PS are directly related to the amount of ionic groups in the P(VDF-*co*-HFP)-*g*-PSSA membranes because sufficient sulfonation can provide sulfonate groups for almost all of the grafted PS monomers. Table 1 summarizes the properties of the P(VDF-*co*-HFP)-*g*-PSSA membranes obtained from the base polymer films with three different thicknesses. They exhibited almost identical IEC, water uptake, and ionic conductivity, as expected from their comparable DOG values.

The thickness of the base polymer films largely increased via radiation grafting and hydration as shown in Figure 2a. Through radiation grafting, the P(VDF-*co*-HFP) films with thicknesses of 100, 200, and 550 μm were converted into the P(VDF-*co*-HFP)-*g*-PSSA membranes with thicknesses of 170, 300, and 800 μm, respectively, when dehydrated. Hydration also induced the increase in the thickness of each membrane, up to 260, 530, and 1280 μm, respectively.

In principle, radicals are evenly generated in the entire region of the base polymer films by γ-ray irradiation. However, as the thickness of the films increases, monomers need a longer time to penetrate through the films and to react with the radicals.[34] For this reason, using a thick base polymer film often leads to the uneven distribution of ionic groups in the membranes obtained via radiation grafting. In other words, the ionic groups might exist mostly on the membrane surface rather than the middle interior region. To inspect the distribution of sulfonate groups, the sulfur profiles through the membrane thickness were observed by using EDS. As shown in Figure 2b, all three membranes including the thickest one (TK) displayed the uniform distribution of sulfur, thus indicating an identical amount of sulfonate groups per unit volume in these membranes.

The structure of ionic clusters in the prepared membranes was observed with SAXS measurements. While previous research has reported the existence of ionic clusters in radiation-grafted ion-exchange membranes,[35,36] the X-ray diffraction by ionic clusters was not found for the P(VDF-*co*-HFP)-*g*-PSSA membranes in this study (Figure S2 in the Supporting Information). This might be due to the irregular distribution of sulfonate groups in the membranes, leading to the absence of X-ray diffraction peaks. Nonetheless, the P(VDF-*co*-HFP)-*g*-PSSA membranes exhibited high ionic conductivity, indicating facile transport of hydrated ions through the membranes. Consequently, it was expected that the performance of IPMC actuators is not largely affected by the irregular distribution of ionic groups.

3.3. Properties of Stacked Nafion Films. Stacking pre-extruded ion-exchange membranes is a simple and reproducible method to obtain ion-exchange membranes with controlled thickness. However, in previous research, stacking Nafion films have been used based on empirical knowledge.[18,37] In this study, an optimized procedure for stacking Nafion films was designed by systematic analyses, and the property variation of the resulting films was examined.

Figure 3a describes the thermal properties of pre-extruded Nafion films. The TGA curve shows the mass change of the Nafion films as a function of increasing temperature. At temperatures below 250 °C, the mass loss was mainly caused by

DOI: 10.1021/acsami.5b04296
ACS Appl. Mater. Interfaces 2015, 7, 16659−16667

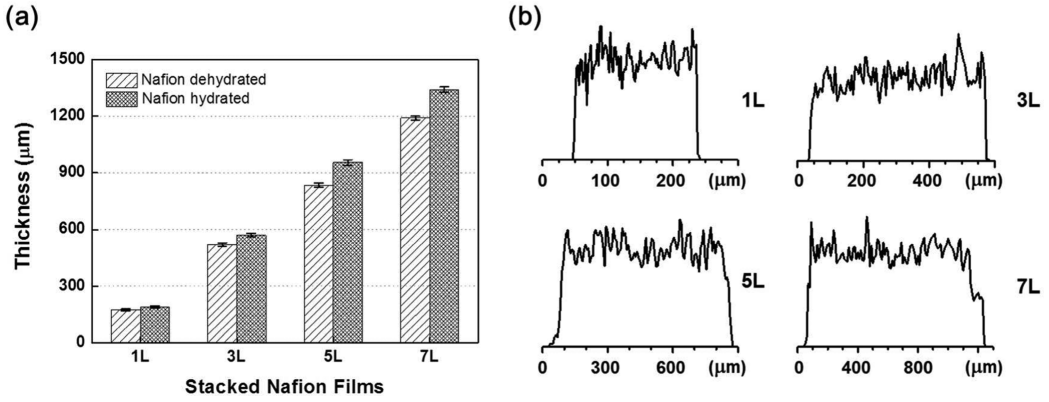

Figure 4. (a) Thickness of stacked Nafion films with a different stacking number of Nafion layers when dehydrated and hydrated. (b) Sulfur profiles through the thickness of the stacked Nafion films.

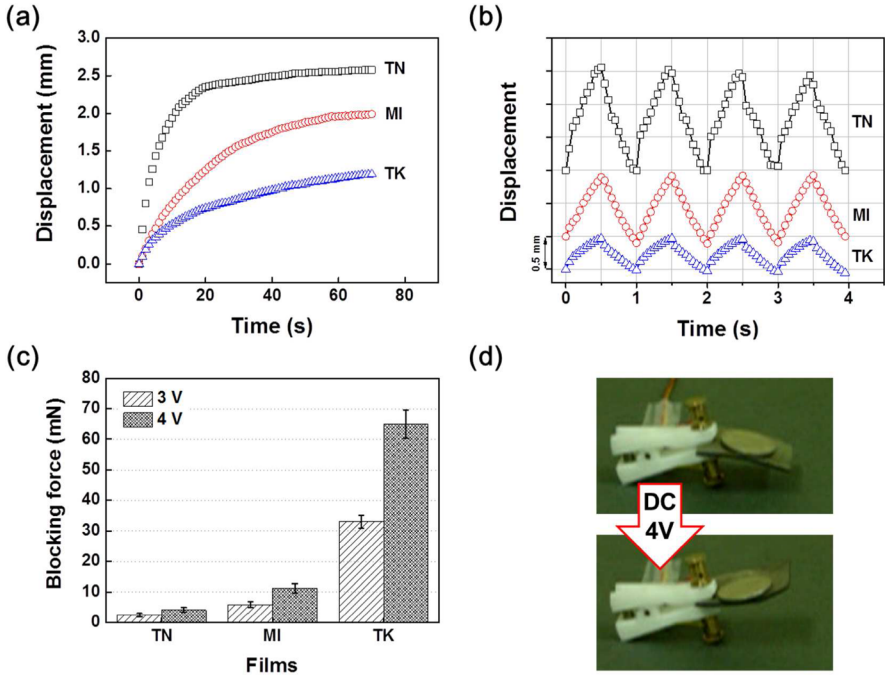

Figure 5. Actuation performance of IPMCs based on P(VDF-*co*-HFP)-*g*-PSSA membranes. Time−displacement curves of the IPMCs measured (a) at a point of 10 mm away from the grip with 2 V of DC and (b) at a point of 20 mm away from the grip with 3 V of AC in the form of a step wave at a frequency of 1 Hz. The thicknesses of TN, MI, and TK IPMCs were about 280, 550, and 1300 μm, respectively. (c) Blocking force of the IPMCs with different thicknesses recorded with a load cell at a point of ∼15 mm away from the grip under 3 and 4 V of DC. (d) Actuation test of the TK IPMCs with a size of 30 × 40 mm^2 under 4 V of DC for 20 s. The weight of the coin was about 7.7 g.

the removal of water that was bound to the ionic groups in the films. However, the degradation of the material, such as desulfonation and decomposition, was distinctly observed over 300 °C.[38−40] In the DSC experiment, the ionic clusters in the Nafion films exhibited transition behaviors over 140 °C,[38−40] which are necessary to connect the ionic clusters between the stacked films for ion transport through the whole films. The crystalline regions of Nafion films melted at around 230 °C.[38−40] However, the fully melted films brought about the flowing of the material during the stacking procedure, causing trouble in controlling the thickness of the resulting films. Because Nafion films at around 190 °C were not entirely melted but softened, pressing allowed them to be completely combined together. Indeed, when observing the cross-sectional image of the membrane stacked with 5 layers of Nafion 117 films at 190 °C (Figure S3 in the Supporting Information), the interfacial layers between the stacked films were not found. To examine the change in the chemical structure of Nafion films due to the stacking process, Raman spectroscopy was utilized.[41] As shown in Figure 3b, the stacked Nafion film (5L) showed an identical Raman spectrum with that of the pristine film (1L), implying the appropriateness of the stacking process.

The thickness of the processed Nafion films was proportionally increased with a number of stacking layers (Figure 4a): the thickness of the 1L, 3L, 5L, and 7L films was 190, 570, 955, and 1340 μm, respectively, when they were hydrated. Figure 4b displays the sulfur profiles through the thickness of the Nafion films. The stacked films (3L, 5L, and 7L) exhibited the uniform distribution of sulfur which is the same as that of the pristine film (1L). The stacking process enables the resulting Nafion films with different thicknesses to have almost identical properties including water uptake, IEC, and ionic conductivity

DOI: 10.1021/acsami.5b04296
ACS Appl. Mater. Interfaces 2015, 7, 16659−16667

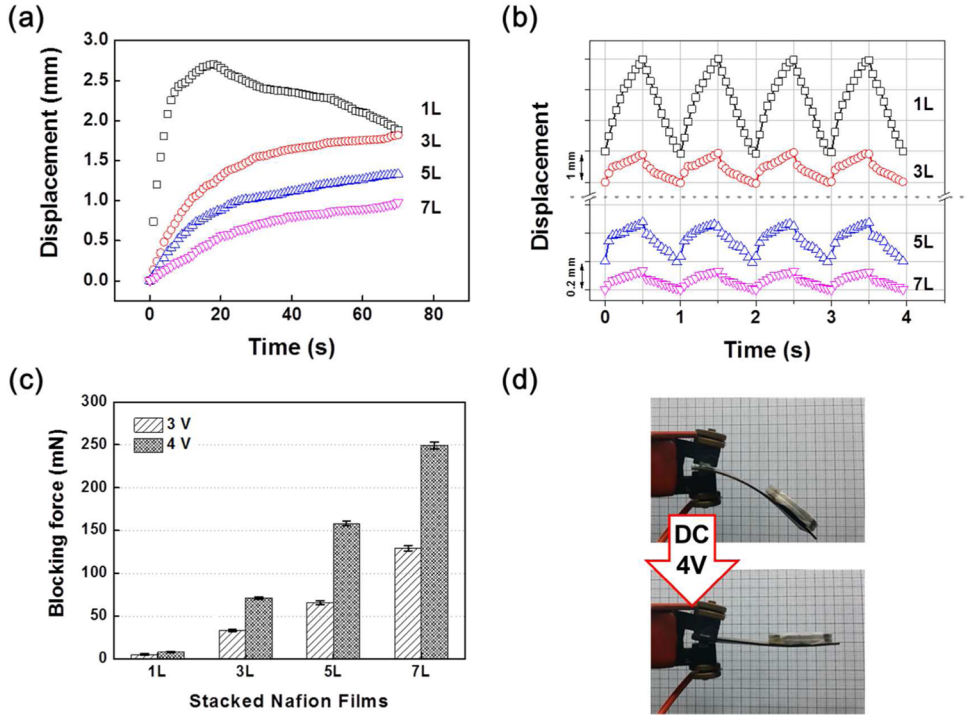

Figure 6. Actuation performance of IPMCs based on stacked Nafion films. Time–displacement curves of the IPMCs measured (a) at a point of 10 mm away from the grip with 3 V of DC and (b) at a point of 20 mm away from the grip with 4 V of AC in the form of a step wave at a frequency of 1 Hz. The curves under AC potentials were plotted with different scales, 1 mm for 1L and 3L IPMCs and 0.2 mm for 5L and 7L IPMCs as shown in b. The thicknesses of 1L, 3L, 5L, and 7L IPMCs were about 210, 590, 975, and 1360 μm, respectively. (c) Blocking force of the IPMCs with different thicknesses recorded with a load cell at a point of ~15 mm away from the grip under 3 and 4 V of DC. (d) Actuation test of the 5L IPMCs with a size of 20 × 60 mm^2 under 4 V of DC for 20 s. The weight of the coins was about 15.4 g.

(Table 1). The structure of ionic clusters in the Nafion films was also observed with SAXS measurements (Figure S2 in the Supporting Information). As previously reported,[39] the pristine Nafion film had the ionic clusters with a size of about 4.41 nm. The stacked films (5L) showed ionic clusters with an almost identical size (4.24 nm). It means that the stacking process hardly changes the structure of the ionic clusters, and thus, the ion transport through the membranes will not be disturbed by the interfaces between the stacked layers. Therefore, it was concluded that the proposed stacking procedure for Nafion films is effective to manipulate the thickness of ion-exchange membranes without any variation of other membrane properties.

3.4. Performance of IPMC Actuators with Different Thicknesses. The IPMC actuators were fabricated from both ion-exchange membranes obtained via radiation grafting and stacking Nafion films. Through a common reduction method,[2,4,42] platinum layers with a thickness of ~10 μm were formed onto both surfaces of all ion-exchange membranes, regardless of the membrane thickness. In this manner, the difference in the platinum layers was minimized, which may affect the performance of IPMC actuators.

Figure 5 describes the actuation performance of P(VDF-*co*-HFP)-*g*-PSSA membrane-based IPMCs. The total thickness containing platinum layers in the IPMCs obtained from TN, MI, and TK membranes was 280, 550, and 1300 μm, respectively. As the thickness increased, the displacement of the IPMCs decreased; when a DC voltage of 2 V was applied for 70 s, the maximum displacements of the three IPMCs were approximately 2.6, 2.0, and 1.2 mm. In addition, applying an AC voltage of 3 V at a frequency of 1 Hz to the IPMCs resulted in the peak displacements of about 1.55, 0.91, and 0.46 mm. However, the force generation of the IPMC actuators was significantly enhanced through increasing the thickness. As shown in Figure 5c, the thick (TK) IPMC generated ~15 times larger force compared to that of the thin (TN) IPMC. The blocking force of the TK IPMC was 65.0 mN at 4 V DC, which enabled the TK IPMC actuator with a size of 30 × 40 mm^2 to lift a coin of 7.7 g (Figure 5d).

The performance of the stacked Nafion film-based IPMC actuators is presented in Figure 6. The IPMCs prepared with 1, 3, 5, and 7 stacking layers of Nafion films had a thickness of 210, 590, 975, and 1360 μm, respectively. For 1L, 3L, 5L, and 7L IPMCs, the propensity in actuation properties was identical to that of P(VDF-*co*-HFP)-*g*-PSSA membrane-based IPMCs: highly improved force generation but decreased displacement as the thickness increased. For the 7L IPMC, the blocking force at DC 4 V was about 250 mN, which was over 30 times larger compared to that of the 1L IPMC. Moreover, two coins of about 15.4 g were successfully lifted by applying a DC voltage of 4 V to the 5L IPMC actuator with a size of 20 × 60 mm^2.

The decrease in the displacement of IPMCs, as their thickness increased, can be explained by the following reasons. For thick IPMCs, the distance that the hydrated mobile ions in the IPMCs have to move is longer than that of thin IPMCs. While the applied electric potential is fixed, the gap between the metal electrodes increases in thick IPMCs. It induces the decrease in effective potential across IPMCs as the thickness increased, causing the slowdown of the movement in mobile ions. Hence, thick IPMCs exhibit relatively slow and small deflection compared to thin IPMCs.

DOI: 10.1021/acsami.5b04296
ACS Appl. Mater. Interfaces 2015, 7, 16659–16667

This supposition can be supported by the time-displacement curves as shown in Figure 6a. The 1L IPMC showed back-relaxation, which often arises from Nafion-based IPMCs because of the back-diffusion of water.[43] However, for the other IPMCs that were relatively thick, back-relaxation was not observed. This is presumably due to the long distance and the reduced electric potential of thick IPMCs causing slow transport of the hydrated mobile ions and preventing the back-diffusion of water.

3.5. Force Generation of IPMCs. From the actuation tests, it was observed that a large blocking force is generated by IPMC actuators with increased thickness. This is because thicker IPMCs can provide a larger bending stiffness. Thus, the relationship between the thickness and bending stiffness of IPMCs needs to be investigated to be able to improve their actuation performance. The bending stiffness is described as the product of Young's modulus and the momentum of inertia of IPMCs. On the basis of the cantilever beam model, the following equation can be obtained.[44]

$$E \cdot I = \frac{PL^3}{3\delta} \tag{1}$$

where P is the applied force, δ is the deflection, L is the length, E is Young's modulus, and I is the momentum of inertia of IPMCs. Because IPMCs have the shape of a rectangular beam, the momentum of inertia is obtained as follows:[44]

$$I = \frac{bh^3}{12} \tag{2}$$

where b is the width, and h is the thickness of the IPMCs. Thus, the Young's modulus of IPMCs is expressed as follows:

$$E = \frac{4PL^3}{\delta bh^3} \tag{3}$$

Using Nafion film-based IPMCs of different stacking layers, the bending stiffness and Young's modulus as a function of the thickness were experimentally evaluated. For the measurements, one end of IPMCs was fixed, and an external force was applied to the other end (30 mm away from the grip) by using a load cell. In other words, the IPMCs were deflected only by a load cell without applying an electric potential. The applied force and the deflection of IPMCs were recorded with a load cell and a laser displacement meter, respectively.

Figure 7 exhibits Young's modulus and bending stiffness as a function of the thickness of stacked Nafion film-based IPMCs. The Young's modulus slightly decreases when the thickness increases. It is due to the relatively increased water content in thick IPMCs because thick films naturally have large inner and small surface portions compared to thin ones, leading to containing more water in the thick films. Indeed, the water uptake of Nafion films gradually increased with increasing thickness (Table 1). It has been reported that the large water content in Nafion films causes the decrease in Young's modulus.[45] The other reason why the Young's modulus is low for thick IPMCs may be related to the decrease in the portion of platinum layers in thick IPMCs because the Young's modulus of Nafion is lower than that of the platinum layers. The thickness of platinum layers on both surfaces was ~20 μm, which was ~9.5% of the total thickness for the 1L IPMC. However, the thickness portion of platinum layers in the 7L IPMC was only ~1.5%.

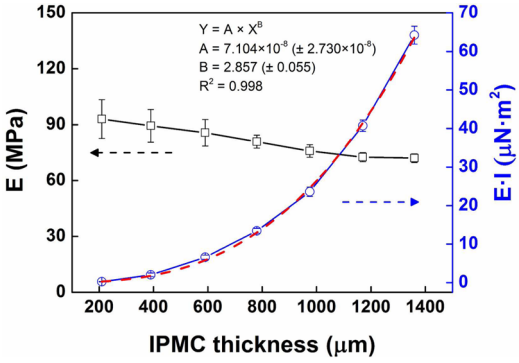

Figure 7. Young's modulus (black square) and bending stiffness (blue circle) as a function of the thickness of stacked Nafion film-based IPMCs. Some error bars are not shown because they are smaller than the size of the data points. The relationship between the bending stiffness and thickness of IPMCs was derived by fitting (red dashed curve) with an equation in the plot.

The bending stiffness highly increased with increasing thickness (Figure 7). The relationship between the two parameters was derived by fitting the values in the bending stiffness to a power function of the thickness. As a result, it was confirmed that the bending stiffness of IPMCs is approximately proportional to the cube (~2.857) of the thickness (h). The reason why the power value is actually lower than 3 is due to the decrease of the Young's modulus for thick IPMCs. Nonetheless, the increase in the bending stiffness with increasing thickness is exceptional, implying that the thicker IPMCs provide a larger force generation.

On the basis of these results, IPMC actuators that generate a large force which is applicable to practical uses were fabricated. The thickness of IPMCs increased up to about 2300 μm by using an ion-exchange membrane prepared via stacking 12 layers of Nafion 117 films. Then, the ultrathick IPMC was utilized to verify how many coins it was possible to lift. Figure 8

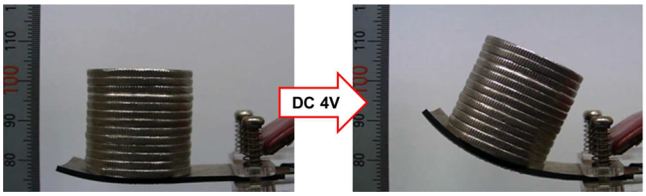

Figure 8. Actuation of IPMC actuator prepared via stacking 12 layers of Nafion 117 films under 4 V of DC for 30 s. The dimension of the IPMC was 20 × 60 × 2.3 mm^3. The total weight of the coins was about 100 g.

shows the actuation of the ultrathick IPMC. When a DC voltage of 4 V was applied to the IPMC actuator with a size of 2 × 6 cm^2, 13 coins (~100 g) were successfully lifted, which had never been demonstrated in previous research. This IPMC actuator with a significantly enhanced force generation will hold important implications in developing artificial muscles.

4. CONCLUSIONS

We have demonstrated that manipulating the thickness of IPMC actuators offers key benefits to enhance their force generation. IPMCs with controlled thickness could be obtained by using ion-exchange membranes prepared via radiation-induced graft copolymerization or stacking of pre-extruded

DOI: 10.1021/acsami.5b04296
ACS Appl. Mater. Interfaces 2015, 7, 16659−16667

films. Because the produced membranes had identical properties but different thicknesses, the effect of IPMC thickness on the actuation performance could be precisely analyzed. The IPMC actuators exhibited a highly enhanced force generation with increasing thickness, resulting from a larger bending stiffness of thicker IPMCs. On the basis of these results, an ultrathick IPMC actuator which can lift a weight of 100 g was fabricated, which showed great potential in developing artificial muscles. These results will be of importance in expanding the applicability of IPMC actuators.

■ ASSOCIATED CONTENT

Supporting Information

Photograph and schematic diagram of a laser displacement meter incorporated with a load cell; small-angle X-ray scattering curves for radiation-grafted ion-exchange membranes and Nafion films; and cross-sectional images of a stacked Nafion film and an ionic polymer−metal composite prepared with the film. The Supporting Information is available free of charge on the ACS Publications website at DOI: 10.1021/acsami.5b04296.

■ AUTHOR INFORMATION

Corresponding Authors

*(J.H.P.) E-mail: hyuk0326@kist.re.kr.
*(J.Y.J.) E-mail: jyjho@snu.ac.kr.

Notes

The authors declare no competing financial interest.

■ ACKNOWLEDGMENTS

This work was supported by the Public Welfare & Safety Research Program through the National Research Foundation of Korea funded by the Ministry of Science, ICT & Future Planning (Grant 2010-0020455). We also acknowledge the financial support from the R&D Convergence Program of National Research Council of Science and Technology of Republic of Korea and a Korea Institute of Science and Technology internal project.

■ REFERENCES

(1) Bar-Cohen, Y. *Electroactive Polymer (EAP) Actuators as Artificial Muscles: Reality, Potential, and Challenges*; SPIE Press: Bellingham, WA, 2001.

(2) Shahinpoor, M.; Bar-Cohen, Y.; Simpson, J. O.; Smith, J. Ionic Polymer−Metal Composites (IPMCs) as Biomimetic Sensors, Actuators and Artificial Muscles−a Review. *Smart Mater. Struct.* **1998**, *7*, R15−R30.

(3) Shahinpoor, M.; Kim, K. J. Ionic Polymer−Metal Composites: I. Fundamentals. *Smart Mater. Struct.* **2001**, *10*, 819−833.

(4) Kim, K. J.; Shahinpoor, M. Ionic Polymer−Metal Composites: II. Manufacturing Techniques. *Smart Mater. Struct.* **2003**, *12*, 65−79.

(5) Nemat-Nasser, S. Micromechanics of Actuation of Ionic Polymer−Metal Composites. *J. Appl. Phys.* **2002**, *92*, 2899−2915.

(6) Tiwari, R.; Garcia, E. The State of Understanding of Ionic Polymer Metal Composite Architecture: A Review. *Smart Mater. Struct.* **2011**, *20*, 083001.

(7) Jo, C.; Pugal, D.; Oh, I.-K.; Kim, K. J.; Asaka, K. Recent Advances in Ionic Polymer−Metal Composite Actuators and Their Modeling and Applications. *Prog. Polym. Sci.* **2013**, *38*, 1037−1066.

(8) Shahinpoor, M.; Kim, K. J. The Effect of Surface-Electrode Resistance on the Performance of Ionic Polymer−Metal Composite (IPMC) Artificial Muscles. *Smart Mater. Struct.* **2000**, *9*, 543−551.

(9) Kim, S.-M.; Kim, K. J. Palladium Buffer-Layered High Performance Ionic Polymer−Metal Composites. *Smart Mater. Struct.* **2008**, *17*, 035011.

(10) Palmre, V.; Pugal, D.; Kim, K. J.; Leang, K. K.; Asaka, K.; Aabloo, A. Nanothorn Electrodes for Ionic Polymer−Metal Composite Artificial Muscles. *Sci. Rep.* **2014**, *4*, 6176.

(11) Lee, D. Y.; Park, I.-S.; Lee, M.-H.; Kim, K. J.; Heo, S. Ionic Polymer−Metal Composite Bending Actuator Loaded with Multi-Walled Carbon Nanotubes. *Sens. Actuators, A* **2007**, *133*, 117−127.

(12) Lian, Y.; Liu, Y.; Jiang, T.; Shu, J.; Lian, H.; Cao, M. Enhanced Electromechanical Performance of Graphite Oxide-Nafion Nanocomposite Actuator. *J. Phys. Chem. C* **2010**, *114*, 9659−9663.

(13) Jung, J.-H.; Jeon, J.-H.; Sridhar, V.; Oh, I.-K. Electro-Active Graphene−Nafion Actuators. *Carbon* **2011**, *49*, 1279−1289.

(14) Jung, J.-H.; Vadahanambi, S.; Oh, I.-K. Electro-Active Nanocomposite Actuator Based on Fullerene-Reinforced Nafion. *Compos. Sci. Technol.* **2010**, *70*, 584−592.

(15) Nam, J.-D.; Lee, J. H.; Choi, H. R.; Kim, H. M.; Jeon, J. W.; Paquette, J.; Kim, K. J.; Tak, Y. S.; Xu, H. Development of Electroactive Silicate Nanocomposites Prepared for Use as Ionic Polymer−Metal Composites (IPMCs) Artificial Muscles and Sensors. *Proc. SPIE* **2002**, *4695*, 387−394.

(16) Nguyen, V. K.; Lee, J. W.; Yoo, Y. Characteristics and Performance of Ionic Polymer−Metal Composite Actuators Based on Nafion/Layered Silicate and Nafion/Silica Nanocomposites. *Sens. Actuators, B* **2007**, *120*, 529−537.

(17) Kim, B.; Kim, B. M.; Ryu, J.; Oh, I.-H.; Lee, S.-K.; Cha, S.-E.; Pak, J. Analysis of Mechanical Characteristics of the Ionic Polymer Metal Composite (IPMC) Actuator Using Cast Ion-Exchange Film. *Proc. SPIE* **2003**, *5051*, 486−495.

(18) Lee, S. J.; Han, M. J.; Kim, S. J.; Jho, J. Y.; Lee, H. Y.; Kim, Y. H. A New Fabrication Method for IPMC Actuators and Application to Artificial Fingers. *Smart Mater. Struct.* **2006**, *15*, 1217−1224.

(19) Duncan, A. J.; Leo, D. J.; Long, T. E. Beyond Nafion: Charged Macromolecules Tailored for Performance as Ionic Polymer Transducers. *Macromolecules* **2008**, *41*, 7765−7775.

(20) Nemat-Nasser, S.; Wu, Y. X. Comparative Experimental Study of Ionic Polymer−Metal Composites with Different Backbone Ionomers and in Various Cation Forms. *J. Appl. Phys.* **2003**, *93*, 5255−5267.

(21) Onishi, K.; Sewa, S.; Asaka, K.; Fujiwara, N.; Oguro, K. The Effects of Counter Ions on Characterization and Performance of a Solid Polymer Electrolyte Actuator. *Electrochim. Acta* **2001**, *46*, 1233−1241.

(22) Asaka, K.; Fujiwara, N.; Oguro, K.; Onishi, K.; Sewa, S. State of Water and Ionic Conductivity of Solid Polymer Electrolyte Membranes in Relation to Polymer Actuators. *J. Electroanal. Chem.* **2001**, *505*, 24−32.

(23) Kim, K. J.; Shahinpoor, M. A Novel Method of Manufacturing Three-Dimensional Ionic Polymer−Metal Composites (IPMCs) Biomimetic Sensors, Actuators and Artificial Muscles. *Polymer* **2002**, *43*, 797−802.

(24) Lee, S.-G.; Park, H.-C.; Surya, D. P.; Yoo, Y. Performance Improvement of IPMC (Ionic Polymer Metal Composites) for a Flapping Actuator. *Int. J. Control Autom. Syst.* **2006**, *4*, 748−755.

(25) Han, M. J.; Park, J. H.; Lee, J. Y.; Jho, J. Y. Ionic Polymer−Metal Composite Actuators Employing Radiation-Grafted Fluoropolymers as Ion-Exchange Membranes. *Macromol. Rapid Commun.* **2006**, *27*, 219−222.

(26) Park, J. H.; Han, M. J.; Song, D. S.; Jho, J. Y. Ionic Polymer−Metal Composite Actuators Obtained from Radiation-Grafted Cation- and Anion-Exchange Membranes. *ACS Appl. Mater. Interfaces* **2014**, *6*, 22847−22854.

(27) Woo, Y.; Oh, S. Y.; Kang, Y. S.; Jung, B. Synthesis and Characterization of Sulfonated Polyimide Membranes for Direct Methanol Fuel Cell. *J. Membr. Sci.* **2003**, *220*, 31−45.

(28) Bhattacharya, A. Radiation and Industrial Polymers. *Prog. Polym. Sci.* **2000**, *25*, 371−401.

DOI: 10.1021/acsami.5b04296
ACS Appl. Mater. Interfaces 2015, 7, 16659−16667

(29) Clough, R. L. High-Energy Radiation and Polymers: A Review of Commercial Processes and Emerging Applications. *Nucl. Instrum. Methods Phys. Res., Sect. B* **2001**, *185*, 8−33.
(30) Dargaville, T. R.; George, G. A.; Hill, D. J. T.; Whittaker, A. K. High Energy Radiation Grafting of Fluoropolymers. *Prog. Polym. Sci.* **2003**, *28*, 1355−1376.
(31) Forsythe, J. S.; Hill, D. J. T. The Radiation Chemistry of Fluoropolymers. *Prog. Polym. Sci.* **2000**, *25*, 101−136.
(32) Nasef, M. M.; Saidi, H.; Dessouki, A. M.; El-Nesr, E. M. Radiation-Induced Grafting of Styrene onto Poly(tetrafluoroethylene) (PTFE) Films. I. Effect of Grafting Conditions and Properties of the Grafted Films. *Polym. Int.* **2000**, *49*, 399−406.
(33) Ma, C.-H.; Yu, T. L.; Lin, H.-L.; Huang, Y.-T.; Chen, Y.-L.; Jeng, U.-S.; Lai, Y.-H.; Sun, Y.-S. Morphology and Properties of Nafion Membranes Prepared by Solution Casting. *Polymer* **2009**, *50*, 1764−1777.
(34) Brack, H. P.; Buhrer, H. G.; Bonorand, L.; Scherer, G. G. Grafting of Pre-irradiated Poly(ethylene-*alt*-tetrafluoroethylene) Films with Styrene: Influence of Base Polymer Film Properties and Processing Parameters. *J. Mater. Chem.* **2000**, *10*, 1795−1803.
(35) Hietala, S.; Holmberg, S.; Karjalainen, M.; Nasman, J.; Paronen, M.; Serimaa, R.; Sundholm, F.; Vahvaselka, S. Structural Investigation of Radiation Grafted and Sulfonated Poly(vinylidene fluoride) (PVDF) Membranes. *J. Mater. Chem.* **1997**, *7*, 721−726.
(36) Elomaa, M.; Hietala, S.; Paronen, M.; Walsby, N.; Jokela, K.; Serimaa, R.; Torkkeli, M.; Lehtinen, T.; Sundholm, G.; Sundholm, F. The State of Water and the Nature of Ion Clusters in Crosslinked Proton Conducting Membranes of Styrene Grafted and Sulfonated Poly(vinylidene fluoride). *J. Mater. Chem.* **2000**, *10*, 2678−2684.
(37) Tiwari, R.; Kim, K. J. Disc-Shaped Ionic Polymer Metal Composites for Use in Mechano-Electrical Applications. *Smart Mater. Struct.* **2010**, *19*, 065016.
(38) Stefanithis, I. D.; Mauritz, K. A. Microstructural Evolution of a Silicon Oxide Phase in a Perfluorosulfonic Acid Ionomer by an In Situ Sol−Gel Reaction. 3. Thermal Analysis Studies. *Macromolecules* **1990**, *23*, 2397−2402.
(39) Mauritz, K. A.; Moore, R. B. State of Understanding of Nafion. *Chem. Rev.* **2004**, *104*, 4535−4585.
(40) de Almeida, S. H.; Kawano, Y. Thermal Behavior of Nafion Membranes. *J. Therm. Anal. Calorim.* **1999**, *58*, 569−577.
(41) Gruger, A.; Régis, A.; Schmatko, T.; Colomban, P. Nanostructure of Nafion® Membranes at Different States of Hydration: An IR and Raman Study. *Vib. Spectrosc.* **2001**, *26*, 215−225.
(42) Nemat-Nasser, S.; Li, J. Y. Electromechanical Response of Ionic Polymer−Metal Composites. *J. Appl. Phys.* **2000**, *87*, 3321−3331.
(43) Enikov, E. T.; Seo, G. S. Analysis of Water and Proton Fluxes in Ion-Exchange Polymer−Metal Composite (IPMC) Actuators Subjected to Large External Potentials. *Sens. Actuators, A* **2005**, *122*, 264−272.
(44) Young, W.; Budynas, R.; Sadegh, A. *Roark's Formulas for Stress and Strain*; 8th ed.; McGraw-Hill Education: New York, 2011.
(45) Satterfield, M. B.; Majsztrik, P. W.; Ota, H.; Benziger, J. B.; Bocarsly, A. B. Mechanical Properties of Nafion and Titania/Nafion Composite Membranes for Polymer Electrolyte Membrane Fuel Cells. *J. Polym. Sci., Part B: Polym. Phys.* **2006**, *44*, 2327−2345.

DOI: 10.1021/acsami.5b04296
ACS Appl. Mater. Interfaces 2015, 7, 16659−16667